GUB Journal of Science and Engineering (GUBJSE)
p-ISSN: 2409-0476
vol. 09, no. 01, 2022

Enhanced SOC estimation in Lithium-ion Batteries using GRU Neural Networks with GSA

Molla Shahadat Hossain Lipu[1], Tuhibur Rahman[2], Naushad Ali[1], Shaheer Ansari[3], Md Sultan Mahmood[4]

1 Department of EEE, Green University of Bangladesh, Dhaka, Bangladesh
2 Department of EEE, Qassim University, Buraydah, Saudi Arabia
3 Department of EEE, Universiti Kebangsaan Malaysia, Bangi, Malaysia
4 Department of EEE, Nagoya University, Nagoya, Japan

*Corresponding author's email:
shahadat@eee.green.edu.bd

Received: 05/06/2022
Accepted: 27/09/2022
Published: 13/07/2024

Data Availability: The data are available on request from the corresponding author.

Competing Interests: The authors declare that they have no known competing financial interests or personal relationships that could have appeared to influence the work reported in this paper.

DOI: 10.3329/gubjse.v9i1.74879

Abstract

State of charge (SOC) is one of the most important metrics to evaluate the performance of the battery management system (BMS) in electric vehicles (EVs). Lithium-ion batteries have been utilized often for SOC estimates in EV applications because of its attractive characteristics such as extended lifespans, high voltages, energy, and capacities. However, dynamic charging and discharging profiles, material degradation, battery aging, chemical reaction, and temperature fluctuations would diverge the accuracy of SOC estimation. Deep learning has proven to become an efficient method for SOC estimation in EVs due to its strong computational capabilities, enhanced generalization performance, and excellent accuracy under dynamic loading profiles. Therefore, this study proposes the use of the gated recurrent unit neural network (GRUNN) for estimating SOC in lithium-ion batteries. The best hyperparameters of GRUNN that enable improving SOC accuracy are found using gravitational search optimization (GSA). To evaluate the functional sustainability of the suggested method, a full battery test bench model is created and accordingly, robustness of the proposed approach is verified under diverse EV drive cycles and aging impacts. The effectiveness of the proposed approach is evaluated by comparing with several existing approaches. The results demonstrate that the suggested method archives SOC error and RMSE in EV driving cycles and ageing effects below 5% and 2%, respectively. The excellent outcomes obtained by the proposed method would certainly enhance the battery charging and discharging profile and EV performance.

Keywords: Electric vehicles, lithium-ion battery, state of charge, algorithm, optimization.

Highlights

- Efficient SOC estimation in EVs using GRU neural networks.
- Robust performance under diverse EV drive cycles and aging effects.
- Achieving SOC error below 5% and RMSE below 2% in testing.

1 Introduction

Globally, the advancement of lithium-ion battery storage system in terms of composition, functionality, cost, and life cycle has drawn the huge attention among the researchers . An extensive investigation has been carried out on the problems and challenges related to state of charge (SOC) assessment, battery charging and discharging control, temperature management, fault diagnostics, and battery protection [1]. The research on batteries with lithium-ion has evolved significantly over the past ten years, notably in China, the United States, South Korea, and Japan, according to the Web of Science (WoS) database, which supports the significance of lithium-ion battery storage systems, as denoted in Fig. 1 [2]. In recent years, there have been a

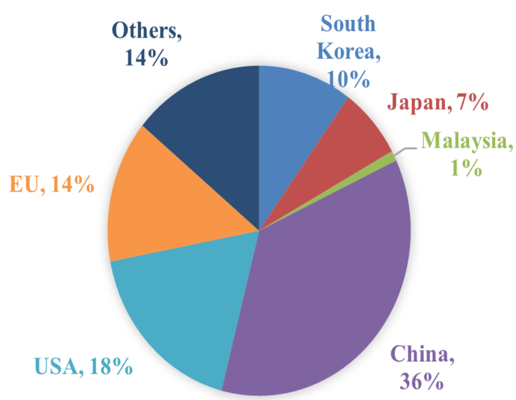

Fig 1. WoS publication on lithium-ion battery storage system

rapid expansion in the applications of lithium-ion battery storage system in the automobile sector due to their increased storage capacity, longer lifespan, and lower cost [3]. Due to its significant potential for reducing the impacts of global warming and carbon emissions, EVs integrated lithium-ion battery storage systems are observed as the promising substitute for diesel-based cars. The EVs have gained popularity as a mode of transportation due to its high engine efficiency, minimal noise production, and zero carbon emissions [4]. The forecast of lithium-ion battery storage system in the automotive industry is presented in Fig. 2 [5].

SOC in BMS has drawn considerable attention for its research impacts in the last decades. SOC stands for the amount of power a lithium-ion battery has delivered to power a vehicle [6]. Battery life is increased and overcharging, over-discharging, and overheating are prevented by

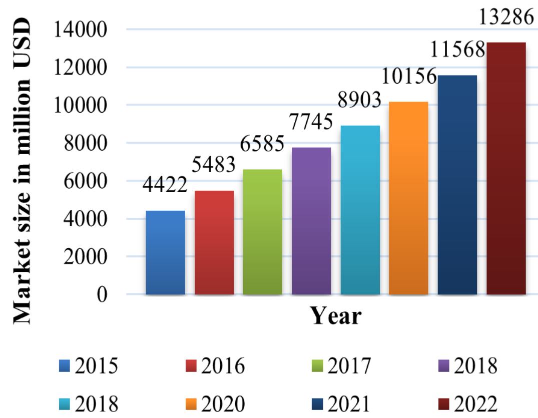

Fig 2. The anticipated use of lithium-ion batteries in EV industry.

using a reliable and accurate SOC assessment technique [7]. Nonetheless, SOC estimation for lithium-ion battery is an internal state that is affected by electrochemical reactions and non-linear properties. Current SOC estimate techniques suffer from several key issues, including temperature fluctuations, sluggish convergence, expensive computations, poor noise tolerance, and the use of an incorrect battery model. To improve the performance of the lithium-ion BMS, an enhanced SOC estimate method must be developed.

2 Theoretical Framework of SOC Algorithm

2.1 Gated Recurrent Unit Network

The gated recurrent unit (GRU) network is a subclass of a recurrent neural network (RNN) with gate characteristics which was introduced in 2014 [8]. For information transmission in the GRU network, a hidden state replaces the cell state. Furthermore, the structure of GRU contains an updating gate, a reset gate, but not a forget gate like the LSTM network does, as shown in Fig. 3. In comparison to the LSTM network, the GRU network has fewer parameters. is described in the following sections. The expression for the update gate is given as:

$$z_t = \sigma \left(W_z \ [h_{t-1}, \ x_k] \right) \tag{1}$$

where W_z is the weight matrix for the update gate and $\sigma()$is the sigmoid activation function. The data for the t-1 units prior is stored in h_{t-1}. By combining $W_z \ [h_{t-1}]$ and

$W_z\ [x_k]$, the result is squeezed between 0 and 1. The revised gate aids the model in selecting the appropriate historical data to be carried forward. The reset gate also decides that the contents of previous information are forgotten. The following is a representation of the reset gate's (r_t) expression:

$$r_t = \sigma\left(W_r\ [h_{t-1},\ x_k] + b_o\right) \quad (2)$$

where the sigmoid activation function $\sigma()$ is present. The reset gate's weight matrix parameter is W_r. The reset gate's bias vector is designated as b_o. The following candidate hidden state (ht), is obtained by integrating the reset gate's output with a typical latent state updating method.

$$\hat{h}_k = \tanh\left(W_o\ [r_t * h_{t-1},\ x_k]\right) \quad (3)$$

where W_o is the weight parameter and $tanh$ is the activation function. Utilizing the Hadamard (elementwise) product operator, the expression is calculated in order to further identify the data that needs to be removed from earlier steps. The network then computes output (h_t), which transmits the data from the current network to the following network. Update gate (z_t) expression is written as,

$$h_t = (1 - z_t) * h_{t-1} + z_t * h_t \quad (4)$$

where z_t is the output of the update gate.

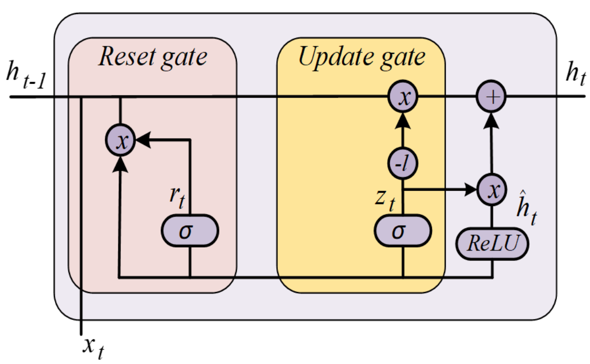

Fig 3. Structure of a gated recurrent unit network

2.2 Gravitational Search Algorithm

GSA is used to find the best solution in any complicated system using the theroy of physics-based computational methods. GSA is superior to other optimization methods in terms of simplicity, quick learning, low training error, and superior generalization performance. Additionally, GSA provides better solutions and does not experience problems such as inappropriate learning rate, local minima, or overfitting.

The motion and law of gravity are applied to form the foundation of GSA. According to the GSA principle, A force is inversely related to the square of the distance between two objects and directly proportional to their masses, as expressed in the following equation [9].

$$F = G\frac{M_1 M_2}{R^2} \quad (5)$$

where F is the gravitational strength, G is the gravitational constant, M1 and M2 are the first and second particles' respective masses, respectively and R is their separation from one another. Newton's second law states the following relationship between a particle's mass, F, force, and acceleration, a:

$$a = \frac{F}{m} \quad (6)$$

The gravitational constant, $G(t_0)$, and the ratio of the initial time t0 and the actual time t0 are used to determine the constant of gravitation, $G\,(t)$

$$G\,(t) = G(t_0) \times \left(\frac{t_0}{t}\right)^{\beta}\ \beta < 1 \quad (7)$$

The positions of the N number of the agents are initialized shown as follows:

$$X_i = \left(X_i^1, \ldots\ldots X_i^d, \ldots\ldots X_i^n\right), \quad \text{for } i = 1, 2, \ldots, N \quad (8)$$

where, n is the space dimension and X_{di} is the position of $i-th$ agent in the $d-th$ dimension. The mathematical expressions for the masses of each agent with regard to the best and worst value are presented as,

$$best\,(t) = minfit_j\,(t) \quad (9)$$

$$Worst\,(t) = maxfit_j\,(t) \quad (10)$$

$$m_i\,(t) = \frac{fit_i\,(t) - Worst\,(t)}{best\ \,(t) - Worst\,(t)} \quad (11)$$

$$M_i\,(t) = \frac{m_i(t)}{\sum_{j=1}^{N} m_i(t)} \quad (12)$$

The velocity, vand position, x are updated using total force F and acceleration,

$$G\,(t) = G_0 e^{(-\alpha t/T)} \quad (13)$$

$$F_{ij}^d\,(t) = G\,(t)\,\frac{M_{pi\times}M_{\alpha j}}{R_{ij} + \varepsilon}\left(X_j^d\,(t) - X_i^d\,(t)\right) \quad (14)$$

$$F_i^d\,(t) = \sum_{j \in Kbest, j \neq i} rand_j F_{ij}^d\,(t) \quad (15)$$

$$a_i^d(t) = \frac{F_i^d(t)}{M_i(t)} \tag{16}$$

$$v_i^d(t+1) = rand_i \times v_i^d(t) + a_i^d(t) \tag{17}$$

$$x_i^d(t+1) = x_i^d(t) + v_i^d(t+1) \tag{18}$$

3 Experimental Arrangement and Data Preparation

3.1 EV Drive Cycle Data

Centre for Advanced Life Cycle Engineering (CALCE) [10] is renowned to conduct the lithium-ion battery experimental tests. In CALCE, various experiments and EV drive cycles dataset are generated. Three popular EV driving cycles such as the Federal Urban Drive Schedule (FUDS), Dynamic Stress Test (DST), and US06 highway drive schedule are employed in this study to test the resilience of the proposed approach. The amplitude and duration of the current profiles for these driving cycles vary widely. A cycle lasts 360, 1372, and 600 seconds for DST, FUDS, and US06, respectively [11]. The current and voltage signals of DST, FUDS, and US06 are recorded in each second to determine SOC at 25°C.

3.2 Battery Experimental Tests

3.2.1 Type of Lithium-ion Battery

In this work, two distinct lithium-ion battery cell chemistries such as lithium nickel cobalt aluminium oxides (LNCA) and lithium nickel manganese cobalt oxides (LNMC) are employed. LNCA uses a Panasonic NCR18650B lithium-ion battery cell. The cathode of this battery is comprised of LiNiCoAlO2, and its rated capacity is 3200 mAh. Maximum discharge current for this battery is 2C (6400 mA). The cut-off voltage is 2.5 V, whereas the usual voltage is 3.6 V [12]. The CC-CV technique, also known as constant current-constant voltage, is used to charge the battery. On the other hand, testing is carried out using Samsung's ICR18650-26F batteries where Graphite serves as the anode and LiNiMnCoO2 (LiNMC) serves as the cathode in the creation of this battery. The test battery has an initial voltage of 3.7 V and a capacity of 2600 mAh. The maximum charging and discharging current are denoted as 2600 mA, and 5200 mA, respectively. The charging voltage and cut-off voltage are assigned as 4.2 V and 2.75 V, respectively [13]. Table 1 presents the specification of lithium-ion batteries that are used for SOC estimation.

Table 1. Lithium-ion Battery Specification

Parameters	$LiNiCoAlO_2$	$LiNiMnCoO_2$
Nominal Capacity (Ah)	3.2	2.6
Nominal Voltage(V)	3.6	3.7
Min/Max Voltage(V)	2.5/4.2	2.75/4.2
Charging Method	CC-CV	CC-CV
Charging Time(hours)	4	3
Charging Current(mA)	1625	1300
Specific Energy (Wh/kg)	200-260	150-220
Lifespan(cycle)	500	1000-2000

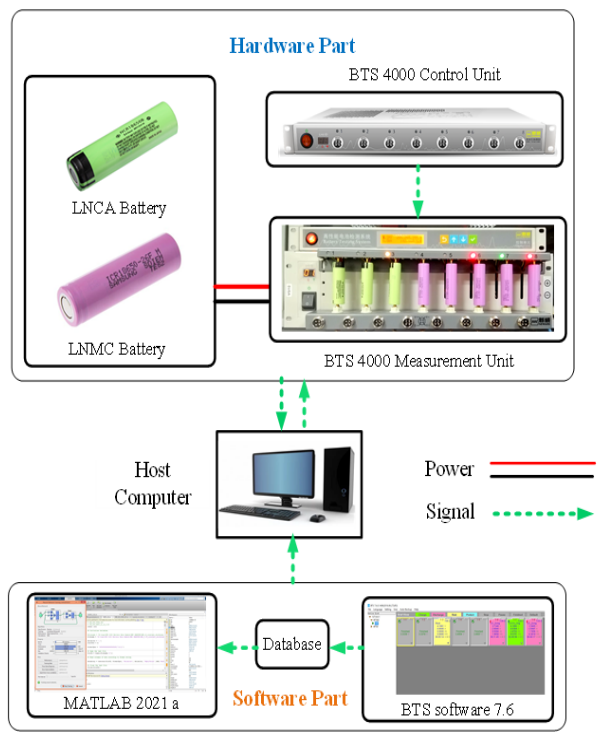

Fig 4. Schematic illustration for test bench model for battery experiments tests

3.2.2 Test Bench Model of Battery

Two components combine to create a test bench model: a hardware component and a software component. Figure 4 displays a schematic representation of the test bench model of lithium-ion batteries for SOC estimation. The NEWARE battery testing system (BTS)-4000, LNCA, and LNMC batteries represent the hardware component. BTS software version 7.6 and MATLAB 2019a are two of the software components that are set up on the host computer. An RS485 port connects the BTS-4000 measurement system, and a TCP/IP port connects to a host computer. Batteries LNCA and LNMC are connected to separate BTS channels. Once the necessary software function has been obtained from BTS software, the lithium-ion battery experiment will begin. The battery experimental test proceeds using the BTS program under various charge and discharge current loads. The LNMC and LNCA battery charging and discharging is controlled by the control unit of the NEWARE BTS-4000 with BTS software version 7.6 while maintaining the threshold of voltage and current scales prescribed by the manufacturer. Then, the MATLAB 2020a program is employed to run the coding and training operation.

3.3 Aging Cycle Test

It is critical to understand how the battery works following a few aging cycles. Typically, when batteries age, their capacity declines. However, different lithium-ion battery types exhibit varied patterns of capacity deterioration. Two aging cycle milestones, 100 and 200 cycles, were selected to test the accuracy and reliability of the approach suggested. The steps of a single aging cycle are shown in Fig. 5. The steps of aging process of lithium-ion battery are explained as follows.

1. Fig. 4. Flowchart CC-CV technique is applied to fully charge the battery.

2. In the case that the battery is fully charged, procedure 3 will start; otherwise, step 1 will repeat.

3. Allow the lithium-ion batteries to rest for 15 minutes.

4. The battery is discharged at a constant rate of 1 C until the battery voltage reaches the lowest cut-off voltage.

5. The lower cut-off voltage of battery is examined. If the battery falls below the minimum threshold value, the aging cycle will stop; otherwise, step 4 will begin again.

6. The battery will rest for one hour after one aging cycle is finished.

7. For the second aging cycle test, step 1 will restart. The process will continue till the predetermined cycles are completed.

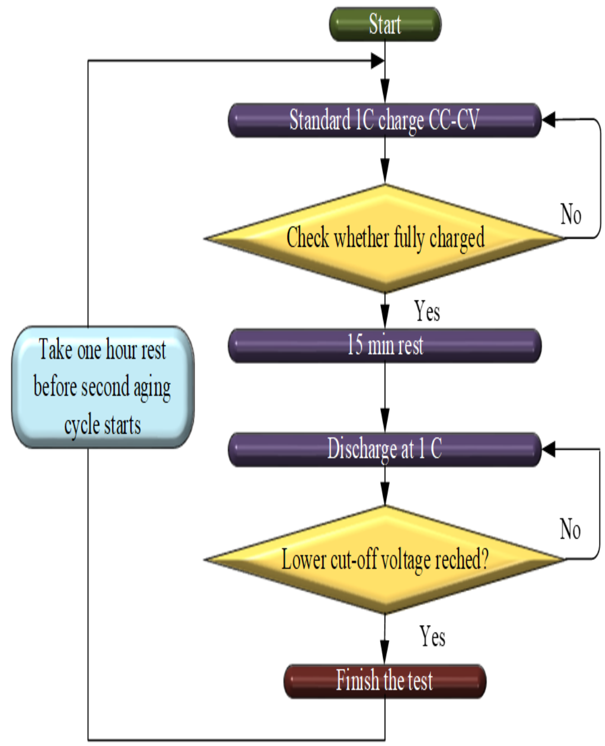

Fig 5. Flowchart of one aging cycle test

3.4 Training and Testing Dataset

The entire dataset is split into two parts such as training and testing after completion of the experimental teats and data measurements. The cross-validation approach is used to divide the data among testing and training phases in a random manner [21]. Through appropriate data normalization, the training data can be strengthened and made more effective. Data normalization has the ability to speed up convergence and remove negative effects., accordingly, the input dataset used in this investigation was normalized to the range [-1,1].

$$a' = \frac{2\,(a - a_{min})}{a_{max} - a_{min}} - 1 \tag{19}$$

where, the maximum and minimum value of input vector a are represented by a_{max} and a_{min}.

3.5 Objective Function and Model Parameter Setting

The objective function of GRUNN is used to determine the lowest possible errors through an iterative process that produces the ideal hyper-parameter values. Due to the large sample size and randomly distributed nature of the SOC error prediction, root means square error (RMSE) was used as the objective function in this study [22]. The following equation is used in establishing the objective function,

$$\text{ObjectiveFunction} = \min(\text{RMSE}) = \min\left(\sqrt{\frac{1}{n}\sum_{i=1}^{n}(SOC_{ai} - SOC_{esi})^2}\right) \quad (20)$$

where, the actual value and the estimated value are denoted by $SOC_a$and SOC_{es}, respectively and n represents the number of observations. The following hyperparameter values of GRUNN are used: learning rate drop factor [0, 1], learning rate drop period [1300], number of hidden layer neurons [50, 200], starting learning rate [0.0001,0.1], number of periods [1000], performance objective [0.000001].

3.6 SOC Performance Evaluation

The effectiveness of the proposed GSA-based GRUNN model is examined using various statistical error terms. The SOC is calculated and compared with the reference value. The mathematical formulas for the different statistical errors are given as follows:

$$SOC\ error = SOC_a - SOC_{es} \quad (21)$$

$$MSE = \frac{1}{n}\sum_{i=1}^{n}(SOC_{ai} - SOC_{esi})^2 \quad (22)$$

$$MAE = \frac{1}{n}\sum_{i=1}^{n}(SOC_{ai} - SOC_{esi}) \quad (23)$$

$$SD = \sqrt{\frac{1}{n-1}\sum_{i=1}^{n}(SOC_{error} - \bar{SOC}_{error})^2} \quad (24)$$

where $\bar{SOC}_{error}$ denotes the average value of SOC error.

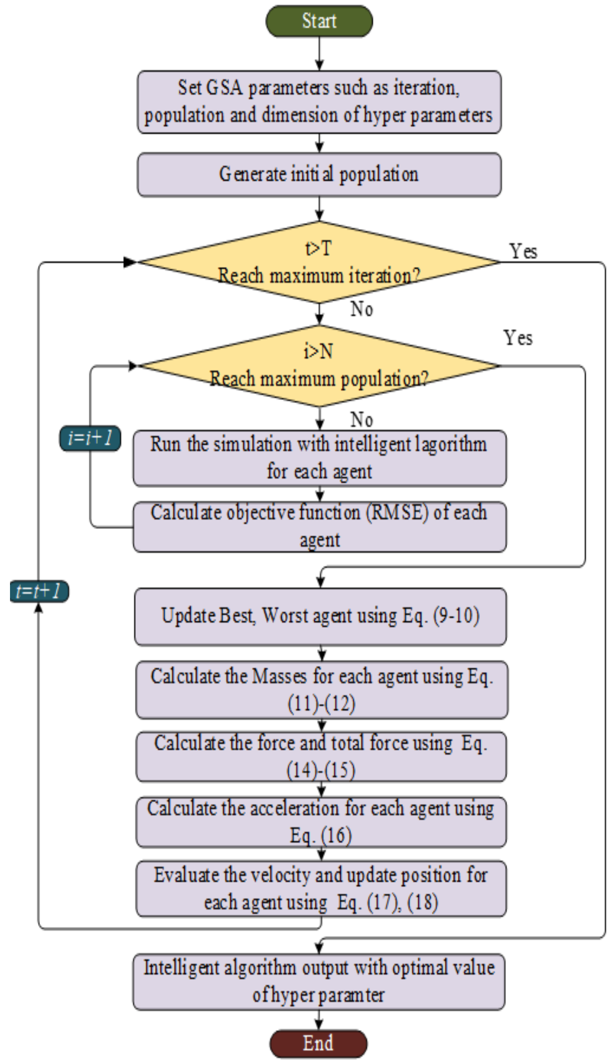

Fig 6. Flowchart of GSA based GRUNN algorithm for SOC estimation

4 Execution of GSA Based Gr Unn Framework for SOC Estimation

The following steps are used for finding the best values of hyper-parameters of GRUNN algorithm using GSA for SOC estimation., as shown in Fig. 6.

1. First, a collection of parameters, including the population size (agent), iteration count, and boundary limit of the hyper-parameters of the GRUNN algorithm, are used to build the GSA algorithm.
2. Hyper-parameters that are positioned inside the boundary range are assigned at random to the location of the agent.
3. GRUNN algorithm training process and activation function are implemented to train the data of hyper-parameters.
4. The objective function of each agent is assessed.
5. The best, and worst position of the agent is updated using equations **??**.
6. The gravitational constant, force, acceleration and velocity of agent are determined using equations **??**,

respectively.

7. The agent velocity and position are updated using expressions **??**.
8. To reassess the objective function of GRUNN, the training process and activation function are both employed.
9. The lowest value of the objective function is used to determine the ideal agent position and velocity. The optimal value of the hyper-parameters is determined by the minimal value of objective function.
10. In the last stage, SOC is calculated using a GRUNN algorithm and the proper hyper-parameter values.

5 Results and Discussions

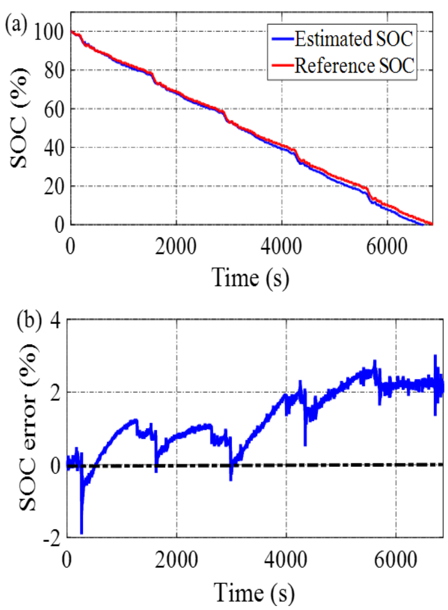

Fig 7. SOC estimation results using FUDS testing and DST training

5.1 SOC Validation Under Diverse EV Drive Cycles

The robustness and generalization capability of the GSA based GRUNN approach for SOC estimation utilizing various testing drive cycles is explained in this section. SOC, SOC error, and various error rates are used to showcase the results. Firstly, DTS driving cycle is used to execute

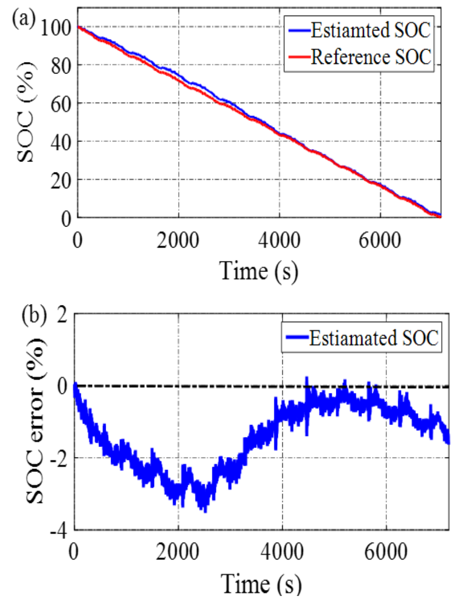

Fig 8. SOC estimation results with DST training and US06 testing

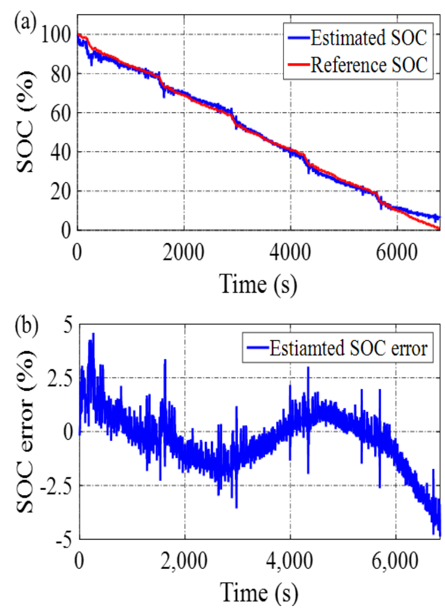

Fig 9. SOC estimate results with US06 training and FUDS testing

the GSA based GRUNN algorithm during training. After that, FUDS drive cycle dataset is used to validate the suggested strategy. It is noticed from Fig.7 that the SOC line under investigation by the GSA based GRUNN approach

Table 2. SOC Performance Assessment in Different Testing Dataset.

Train	Test	RMSE (%)	MSE (%)	MAE (%)	MAPE (%)	SD (%)	SOC error (%)
DST	FUDS	1.5452	0.0239	1.3274	5.1465	1.3287	[- 1.89, 3.18]
DST	US06	1.6264	0.0265	1.4151	5.0289	1.4275	[- 3.23, 0.36]
US06	FUDS	1.7236	0.0428	1.5171	7.0448	2.1223	[- 4.77, 4.59]

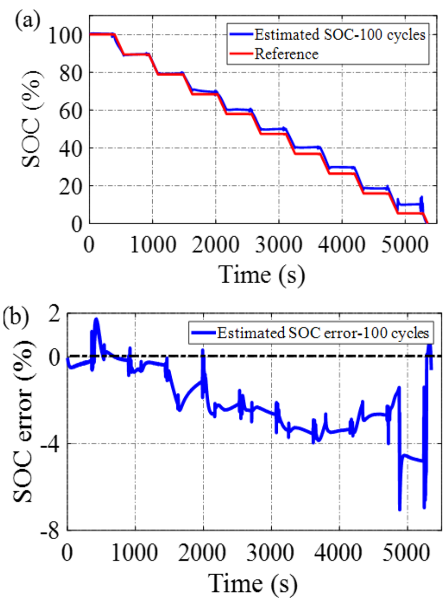

Fig 10. Performance of the LNCA battery after 100 age cycles (a) SOC (b) SOC error.

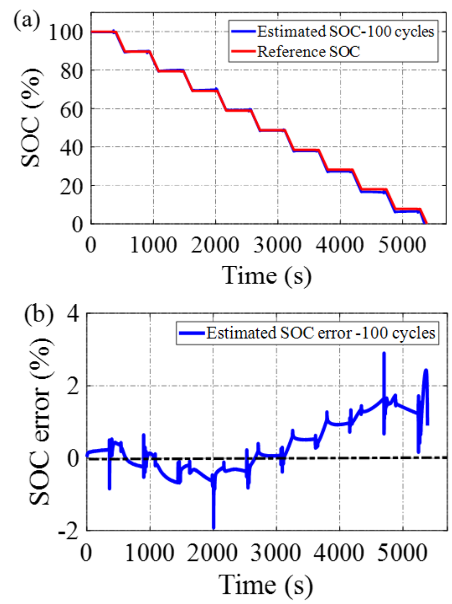

Fig 11. Performance of the LNMC battery after 100 age cycles (a) SOC (b) SOC error.

is identified to be closely matched with the reference SOC values. The SOC error range is limited to [-1.89%, 3.18%].

The adaptability of GSA based GRUNN algorithm is further assessed using DST drive cycle as the training dataset and US06 drive cycle as the testing dataset, as shown in Fig. 8. The findings are satisfactory as the SOC error is minimal, with a range of [-3.53%, 0.26%]. In addition, with RMSE and MAE error rates are estimated to be 1.6574% and 1.4051%, respectively.

In addition, the accuracy of GSA based GRUNN approach for SOC estimation is evaluated with the FUDS drive cycle after training with the US06 drive cycle. The results are satisfactory with the SOC error of [- 4.77%, 4.59%] and RMSE and MAE of 2.125% and 1.5171%, respectively, as denoted in Fig. 9. The findings demonstrate the excellent resilience of the GSA based GRUNN approach against the various testing datasets. As stated in Table 2, the outcomes are evaluated in terms of several performance metrics.

5.2 SOC Estimation Under Aging Cycles

The investigation of the performance of SOC under aging cycles is shown in Figures 10and 11. MAE for a LNMC battery is estimated to be 0.6108% at 100 cycles. In terms of accuracy, the LNMC battery outperforms the LNCA battery, with a SOC error range of [-7.05%, 1.65%] as opposed to [-1.92%, 2.89%] for the LNCA battery.

As shown in Figures 12 and 13, the SOC assessment of LNCA and LNMC batteries is further examined through 200 aging cycles. Deep cycling of a LNCA battery is found to drastically reduce its accuracy. According to the findings, RMSE and SOC error boundaries of LNCA battery were determined to be 3.4814 % and [-9.84%, 9.77%], respectively. on the other hand, LNMC battery provides exceptional SOC estimation results during heavy aging cycle with RMSE and SOC error limits of 1.2876 % and [-4.84%, 4.91%], respectively. Table 3 displays the results of SOC estimation for various EV drive cycles.

Table 3. SOC Estimation under different aging cycles

Aging Cycle	Battery	RMSE (%)	MAE (%)	SD (%)	SOC error (%)
100	LNCA	2.5507	2.1315	2.4658	[-7.05, 1.65]
	LNMC	0.7917	0.6108	0.7845	[-1.92, 2.89]
200	LNCA	3.4814	2.9813	3.3485	[-9.84, 9.77]
	LNMC	1.2876	0.9606	1.2586	[-4.84, 4.91]

Table 4. A comparison between the proposed approach and existing SOC estimation approaches

Method	Refs.	Test battery	Validation Profile	Temperature	Error rate
Recurrent Neural Network (RNN)	[24]	LiFePO4 and LTO	Pulse charging and discharging	0°C, 10°C, 25°C and 40°C	RMSE 0.31% 0.41% for LiFePO4 battery RMSE 0.41% 0.43% for LTO battery
Deep neural network (DNN)	[20]	2.9 Ah Panasonic LiNiCoAlO2	FUDS	0°C, 10°C, and 25°C	MAE 1.85% FUDS
Adaptive neuro fuzzy inference system (ANFIS)	[25]	40 Ah, 36 Lithium-Ion cells	Charging and discharging currents (i) 57 A, (ii) 68 A	Temperature range from -30 °C to 55 °C	MSE 3.4% in 57 A MSE 5.6% in 68A
ANN + UKF	[23]	2.3 Ah LiFePO4	(i) US06 (ii) FUDS	0°C to 50°C	RMSE 2.5% in US06 RMSE 1.4% in FUDS
Proposed approach		LNCA and LNMC	(i) DST (ii) FUDS (iii) US06	25°C	RMSE < 1.7 % in US06 RMSE <1.8% in FUDS

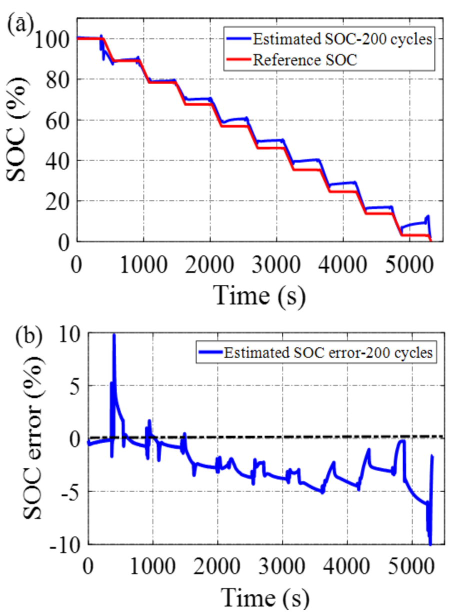

Fig 12. Performance of the LNCA battery after 200 age cycles (a) SOC (b) SOC error.

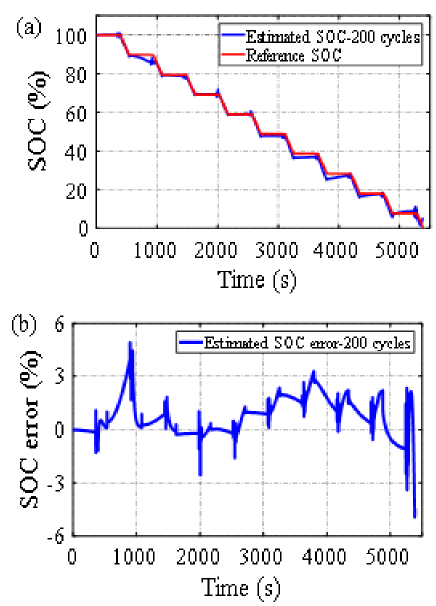

Fig 13. Performance of a LNMC battery after 200 aging cycles (a) SOC (b) SOC error.

5.3 Comparative Analysis

Current state-of-the-art SOC estimation strategies are compared to the GSA-based GRUNN approach to validate the accuracy and resilience, as shown in Table 4. Under a variety of lithium-ion battery types, drive cycles, and temperature conditions, it has been found that the GSA-based GRUNN method for SOC estimation is superior to the existing SOC estimation methods. For instance, deep neural network algorithm computes MAE to be under 2% in FUDS drive cycle [13]. Nevertheless, the proposed method computes RMSE to be below 1.8% in FUDS cycle. In addition, The RMSE of the unscented Kalman filter (UKF) approach based on artificial neural networks (ANN) in the US06 cycle is 2.5 %. [23]. However, the suggested model offers outcomes that are more accurate, with an RMSE of 1.6264% in the US06 cycle.

6 Conclusion

In this study, a GSA based GRUNN approach is proposed to enhance the accuracy of SOC estimation. The best hyperparameters are investigated using GSA, including learning rate, hidden neurons, learning rate drop, and learning rate drop period. Battery aging cycles and various EV driving cycle datasets are used to evaluate the developed model. Under various testing datasets, the robustness of the suggested approach is verified. According to the results, under all drive cycle circumstances, GSA-based GRUNN outperforms exiting SOC estimation methods by achieving a lower error rate, indicating RMSE below 1.8% and SOC error below 5%. Additionally, the suggested model performs efficiently under various aging cycles, with MAE in LNMC and LNCA batteries being under 1% and 3%, respectively. The applicability of the suggested in online BMS applications is further demonstrated by a comparative study using the most recent SOC estimation technique, which demonstrates reduced error rates in comparison to RNN, DNN, ANFIS, and UKF. By creating hardware for the loop test, the suggested work may be expanded even further.

7 Acknowledgements

This paper and the research behind it would not have been possible without the support of Ministry of Science and Technology (MoST) under Project ID SRG- 232384 and Grant for Advanced Research in Education (GARE) scheme, Bangladesh Bureau of Educational Information and Statistics (BANBEIS), Project Code: ET20222235 and Center for Research Innovation and Transformation (CRIT), Green University of Bangladesh, Project ID: G-23-22-14.

References

[1] S. Son, S. Jeong, E. Kwak, J.-h. Kim, and K.-Y. Oh, "Integrated framework for soh estimation of lithium-ion batteries using multiphysics features," *Energy*, vol. 238, p. 121 712, 2022.

[2] M. H. Lipu, M. Hannan, T. F. Karim, *et al.*, "Intelligent algorithms and control strategies for battery management system in electric vehicles: Progress, challenges and future outlook," *Journal of Cleaner Production*, vol. 292, p. 126 044, 2021.

[3] M. H. Lipu, M. Hannan, T. F. Karim, *et al.*, "Intelligent algorithms and control strategies for battery management system in electric vehicles: Progress, challenges and future outlook," *Journal of Cleaner Production*, vol. 292, p. 126 044, 2021.

[4] S. Li, Y. Li, D. Zhao, and C. Zhang, "Adaptive state of charge estimation for lithium-ion batteries based on implementable fractional-order technology," *Journal of Energy Storage*, vol. 32, p. 101 838, 2020.

[5] M. H. Lipu, S. Ansari, M. S. Miah, *et al.*, "Deep learning enabled state of charge, state of health and remaining useful life estimation for smart battery management system: Methods, implementations, issues and prospects," *Journal of Energy Storage*, vol. 55, p. 105 752, 2022.

[6] M. H. Lipu, M. Hannan, A. Hussain, *et al.*, "Differential search optimized random forest regression algorithm for state of charge estimation in electric vehicle batteries," in *2021 IEEE Industry Applications Society Annual Meeting (IAS)*, IEEE, 2021, pp. 1–8.

[7] G. O. Sahinoglu, M. Pajovic, Z. Sahinoglu, Y. Wang, P. V. Orlik, and T. Wada, "Battery state-of-charge estimation based on regular/recurrent gaussian process regression," *IEEE Transactions on Industrial Electronics*, vol. 65, no. 5, pp. 4311–4321, 2017.

[8] M. H. Lipu, M. Hannan, A. Hussain, *et al.*, "Data-driven state of charge estimation of lithium-ion batteries: Algorithms, implementation factors, limitations and future trends," *Journal of Cleaner production*, vol. 277, p. 124 110, 2020.

[9] E. Chemali, P. J. Kollmeyer, M. Preindl, R. Ahmed, and A. Emadi, "Long short-term memory networks for accurate state-of-charge estimation of li-ion batteries," *IEEE Transactions on Industrial Electronics*, vol. 65, no. 8, pp. 6730–6739, 2017.

[10] W. He, N. Williard, C. Chen, and M. Pecht, "State of charge estimation for li-ion batteries using neural network modeling and unscented kalman filter-based error cancellation," *International Journal of Electrical Power & Energy Systems*, vol. 62, pp. 783–791, 2014.

[11] H. Chaoui and C. C. Ibe-Ekeocha, “State of charge and state of health estimation for lithium batteries using recurrent neural networks,” *IEEE Transactions on vehicular technology*, vol. 66, no. 10, pp. 8773–8783, 2017.

[12] J. Chen, Y. Zhang, J. Wu, W. Cheng, and Q. Zhu, “Soc estimation for lithium-ion battery using the lstm-rnn with extended input and constrained output,” *Energy*, vol. 262, p. 125 375, 2023.

[13] M. A. Awadallah and B. Venkatesh, “Accuracy improvement of soc estimation in lithium-ion batteries,” *Journal of Energy Storage*, vol. 6, pp. 95–104, 2016.

Molla Shahadat Hossain Lipu (Senior Member, IEEE) received the B.Sc. degree in electrical and electronic engineering from the Islamic University of Technology, Bangladesh, in 2008, the M.Sc. degree in energy from the Asian Institute of Technology, Thailand, in 2013, and the Ph.D. degree in electrical, electronic and systems engineering from the National University of Malaysia, in 2019. He is currently an Associate Professor with the Department of Electrical and Electronic Engineering, Green University of Bangladesh (GUB). Prior to joining GUB, he worked as a Senior Lecturer with the Department of Electrical, Electronic, and Systems Engineering, National University of Malaysia, and an Assistant Professor with the Department of Electrical and Electronic Engineering, University of Asia Pacific, Bangladesh. He has teaching experience at university for more than ten years in local and foreign universities. He secured a place in the list of the world’s best 2% scientists published by Stanford University and Elsevier, in 2022 and 2023. He published numerous top-notch journals in IEEE Transactions, Elsevier, and Nature Science. His research interests include battery storage and management systems, electrical vehicles, power electronics, intelligent controllers, artificial intelligence, and optimization in renewable systems. He won the best paper award in reputed IEEE conferences and was also awarded the gold medal in several exhibitions. He worked as the Track Chair and a Convener at the 4th International Conference on Sustainable Technologies for Industry 4.0 (STI 2022), organized by GUB. In addition, he worked as an invited speaker, the session chair at conferences, and a reviewer in top-ranked journals. He served as the guest editor for several renowned journals.

Tuhibur Rahman focuses his research in the fields of Renewable Energy, Battery energy storage system, Solar Energy and Sustainability. He acquired his Bachelor Degree in Electrical and Electronics Engineering from Green University of Bangladesh. Currently, he is working as Instructor for Laboratory Courses at Department of Electrical Engineering, Qassim University, Saudi Arabia. He has several publications in renowned journals and also presented his work at prestigious international conferences. Apart from his academic experiences, he served as Chair of IEEE power and Energy Society for the years of 2020-2022 .He was also participated as invited speaker in several IEEE PES events.

M M Naushad Ali has been working as an Assistant Professor of EEE department at Green University of Bangladesh. Besides his full-time academic teaching, he is also functioning as a Program Coordinator. His leadership skill in the academic field is very sturdy and stirring to others. He attended and completed many academic teaching and learning workshops. Mr. Naushad Ali several publications in renowned journals. He has also presented his work at prestigious international conferences. He is an active member of IEEE from his academic life. Mr. Maruf received his B.Sc. degree in Electrical and Electronic Engineering (EEE) from Islamic University of Technology (IUT) Dhaka, Bangladesh in 2008 and an M.Sc in Industrial and Information Systems Engineering from Hankuk University of Foreign Studies (HUFS) Republic of Korea in 2013.

Shaheer Ansari received a B.Sc. degree in electrical and electronic engineering and a master’s degree in instrumentation and control from Integral University, Lucknow. Furthermore, he pursued a Ph.D. degree with the Department of Electrical, Electronic and Systems Engineering, Universiti Kebangsaan Malaysia in the year 2023. Currently, he is working as a postdoctoral researcher in the Department of Electrical, Electronic and Systems Engineering, Universiti Kebangsaan Malaysia. His research interests include machine learning algorithms, optimization schemes for prognostics, and health management.

Md. Sultan Mahmud received the B.Sc. degree in electrical and electronic engineering from the University of Asia Pacific, Bangladesh, in 2014, and the M.Tech. degree in green energy technology from Pondicherry University, India, in 2017. He is currently pursuing the Ph.D. degree in micro-nano mechanical science and engineering with Nagoya University, Japan. He worked as a Lecturer with the Department of Electrical and Electronic Engineering, City University, Bangladesh, from 2017 to 2019. His current research interests include fabrication of nanomaterial through physical method and application of nanomaterial for photocatalytic water splitting.